

Discovery of Pyridyl-Benzothiazol Hybrids as Novel Protoporphyrinogen Oxidase Inhibitors via Scaffold Hopping

Hui Cai, Xiao Zhang, Dan Ling, Meng Zhang, Chen Pang, Zhongyin Chen, Zhichao Jin, Shi-Chao Ren,* and Yonggui Robin Chi*



Cite This: <https://doi.org/10.1021/acs.jafc.3c08596>



Read Online

ACCESS |

Metrics & More

Article Recommendations

Supporting Information

ABSTRACT: In order to discover novel protoporphyrinogen oxidase (PPO) inhibitors with excellent herbicidal activity, a series of structurally novel 6-(pyridin-2-yl) benzothiazole derivatives were designed based on the scaffold hopping strategy. The in vitro experiments demonstrated that the newly synthesized compounds exhibited noteworthy inhibitory activity against *Arabidopsis thaliana* PPO (AtPPO), with IC₅₀ values ranging from 0.06 to 1.36 μM. Preliminary postemergence herbicidal activity tests and crop safety studies indicated that some of our compounds exhibited excellent herbicidal activity and crop safety. For instance, compound (*rac*)-7as exhibited superior herbicidal activities to commercially available flumioxazin (FLU) and saflufenacil (SAF) at all the tested concentrations and showed effective herbicidal activities even at a dosage as low as 18.75 g ai/ha. Meanwhile, compound (*rac*)-7as showed good crop safety for wheat at a dosage as high as 150 g of ai/ha. Although the absolute configuration of compound 7as has no obvious effect on its herbicidal activity, compound (R)-7as showed a slightly higher crop safety than compound (S)-7as. Molecular simulation studies of *Nicotiana tabacum* PPO (NtPPO) and our candidate compounds showed that the benzothiazole moiety of compounds (R)-7as or (S)-7as formed multiple π–π stacking interactions with FAD, and the pyridine ring generated π–π stacking with Phe-392. Our finding proved that the pyridyl–benzothiazol hybrids are promising scaffolds for the development of PPO-inhibiting herbicides.

KEYWORDS: scaffold hopping, pyridyl–benzothiazol hybrids, protoporphyrinogen IX oxidase, herbicides

INTRODUCTION

Protoporphyrinogen oxidase (PPO, EC 1.3.3.4) is a key enzyme in the biosynthesis of chlorophyll, which catalyzes the conversion of protoporphyrinogen IX to protoporphyrin IX in the chloroplasts and mitochondria of plants, therefore making it one of the most important targets for herbicides.^{1–4} Specifically, the activity of PPO is inhibited when plants are treated with PPO herbicides, resulting in the accumulation of protoporphyrinogen IX and the suppression of protoporphyrin IX synthesis, and therefore affects the formation of the chloroplast.^{5–8} Besides, the accumulated protoporphyrinogen IX within the chloroplasts will leak into the cytoplasm, wherein the protoporphyrinogen IX undergoes auto-oxidation to form the protoporphyrin IX. When exposed to light, the protoporphyrin IX in the cytoplasm will promote the formation of reactive oxygen species (ROS) in the presence of oxygen (O₂), which leads to lipid peroxidation and ultimately results in cell death.^{9–11}

Indeed, PPO-inhibiting herbicides have been used for weed control in the field for more than half a century.^{12,13} They are characterized by high efficiency of weed control, favorable environmental safety, low application dosage, and low toxicity to mammals.^{14,15} Besides, the spectrum of weed control for PPO inhibitors is broad, including broadleaf weeds, some grass weeds, and even those that have developed resistance to glyphosate and acetolactate synthase (ALS)-inhibiting herbicides.^{16,17} Consequently, the design and synthesis of new PPO

inhibitors have consistently been a highly active research field in herbicide development.

Over the years, scaffold hopping has been proven to be a powerful strategy for developing new agricultural chemicals due to its advantages in improving the physicochemical properties, enhancing biological activity, and overcoming the narrow intellectual property of lead compounds or old agrochemicals.^{18,19} Among the strategies used for scaffold hopping, heterocycle replacements have been extensively applied in the herbicide optimization process including PPO inhibitor development.²⁰ Due to our continuous interest in developing structurally novel small molecules with agricultural activities, we are interested in designing protoporphyrinogen oxidase (PPO) inhibitors with excellent herbicidal activity under the direction of the scaffold hopping strategy.^{21–23}

Our entry to this objective was in part inspired by pyrimidinedione and phenylpyridine skeletons. Pyrimidinedione is a privileged structure for designing PPO inhibitors with noteworthy examples such as saflufenacil, butafenacil, and tiafenacil (Figure 1a).²⁴ In 2016, Yang's research group also reported a pyrimidinedione-containing compound 9F-6 as a

Received: November 17, 2023

Revised: March 27, 2024

Accepted: March 27, 2024

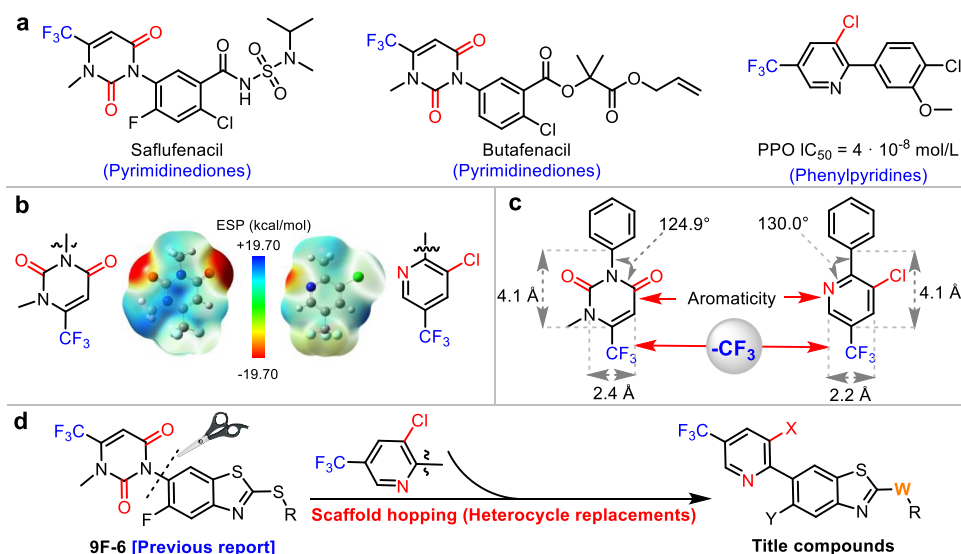


Figure 1. (a) Representative structures of pyrimidinedione and phenylpyridine herbicides; (b) ESP analysis of pyrimidinedione and 3-Cl-5-CF₃-2-pyridyl fragments; (c) chemical space analysis of pyrimidinedione and 3-Cl-5-CF₃-2-pyridyl fragments; (d) design strategy for the target compounds.

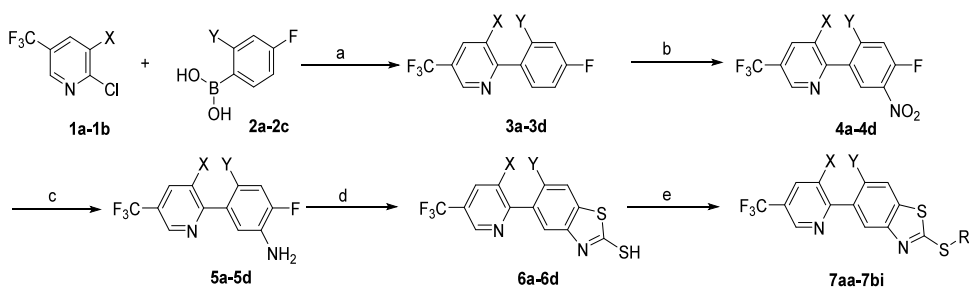


Figure 2. Synthetic route for compounds 7aa–7bi. Reagents and conditions: (a) Pd(PPh₃)₂Cl₂, Na₂CO₃, 1,4-Dioxane/H₂O = 1/1, 60 °C; (b) HNO₃, H₂SO₄, 0 °C - r.t.; (c) Fe, NH₄Cl, C₂H₅OH (80 %), reflux; (d) EtOC(S)SK, DMF, 90 °C, con. HCl; (e) R–X, K₂CO₃, CH₃CN, 50 °C.

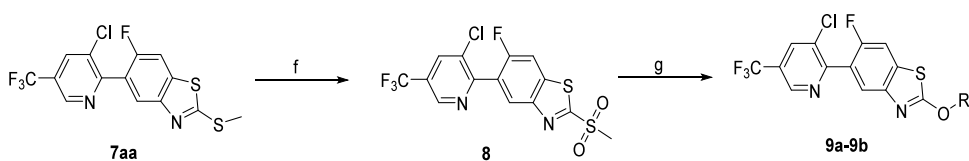


Figure 3. Synthetic procedures of compounds 8, 9a, and 9b. Reagents and conditions: (f) NaIO₄, RuCl₃, CH₃CN, CCl₄, H₂O. (g) R–OH, K₂CO₃, CH₃CN, 50 °C.

typical PPO inhibitor, which exhibits broad-spectrum herbicidal activity at a concentration of 37.5 g ai/ha (Figure 1d).²⁵ On the other hand, phenylpyridine also found applications in PPO inhibitors. For example, Schäfer et al. designed and synthesized a series of novel phenylpyridine compounds under the direction of molecular modeling strategy from diphenyl ethers (Figure 1a), a PPO-inhibiting herbicide. These compounds exhibit strong PPO inhibitory activity (PPO IC₅₀ = 4 × 10^{−8} mol/L) and therefore exhibited good herbicidal activity.²⁶ We found that there are considerable similarities between the pyrimidinedione moiety and the 3-Cl-5-CF₃-2-pyridyl fragment in terms of the electrostatic potential (ESP) and chemical space (Figure 1b,c). For example, both fragments are trifluoromethyl-substituted six-membered *N*-containing aromatic heterocycles, which therefore lead to a similar three-dimensional structure. Besides, ESP calculations suggested that the two fragments bear a considerably similar

ESP, which would result in similar behavior in terms of electrostatic interactions between the ligand and protein.^{27–29}

Based on the above analysis and the scaffold hopping strategy, we herein report that a series of novel PPO inhibitors were designed by replacing the pyrimidinedione fragment of compound 9F-6 with the 3-Cl-5-CF₃-pyridin-2-yl moiety (Figure 1d). A series of 6-(substituted pyridin-2-yl) benzo [d] thiazole derivatives were prepared and studied. In vitro experiments were conducted which proved that our newly designed compounds exhibited noteworthy inhibitory activity against *Arabidopsis thaliana* PPO (AtPPO). Preliminary postemergence herbicidal activity tests and crop safety studies demonstrated that some of our compounds exhibited good herbicidal activities and crop safety. Molecular docking and molecular dynamics (MD) simulation studies were performed to gain insights into the inhibitory mechanism. The excellent herbicidal activities and the high crop safety demonstrated that such types of compounds are potential candidate molecules for

Table 1. Postemergence Herbicidal Activities of Substituted 6-(pyridin-2-yl) Benzothiazole Derivatives

compd	dosage (g ai/ha)	X	Y	W	R	L.P. ^a	E.C.	inhibition (%)			
								D.S.	A.R.	A.T.	M.S.
6a	150	Cl	F	S	H	0	0	0	100	100	80
6b	150	H	F	S	H	0	0	0	40	10	20
6c	150	Cl	Cl	S	H	0	0	0	40	10	20
6d	150	Cl	CH ₃	S	H	0	0	0	30	10	20
7aa	150	Cl	F	S	CH ₃	40	80	100	100	100	100
7ab	150	Cl	F	S	CH ₂ CH ₃	40	40	100	100	100	100
7ac	150	Cl	F	S	CH ₂ CH ₂ CH ₃	40	100	100	100	100	100
	75					30	80	90	100	100	100
	37.5					20	70	75	100	100	100
	18.75					10	60	70	100	100	100
7ad	150	Cl	F	S	CH ₂ CH ₂ CH ₂ CH ₃	40	70	50	100	100	100
7ae	150	Cl	F	S	CH ₂ CH ₂ OH	20	80	70	100	100	100
7af	150	Cl	F	S	CH ₂ CH ₂ Br	20	40	80	100	100	100
7ag	150	Cl	F	S	CH ₂ CH=CH ₂	70	70	70	100	100	100
7ah	150	Cl	F	S	CH ₂ CH=CH(CH ₃) ₂	0	60	80	100	100	100
7ai	150	Cl	F	S	CH ₂ CH=CHCl	0	0	0	100	100	100
7aj	150	Cl	F	S	CH ₂ C≡CH	70	90	100	100	100	100
	75					60	80	100	100	100	100
	37.5					50	70	90	100	100	100
	18.75					40	60	70	100	100	100
7ak	150	Cl	F	S	CH ₂ C≡CCH ₃	0	0	0	100	100	20
7al	150	Cl	F	S	CH ₂ COCH ₂ CH ₃	0	0	0	100	100	40
7am	150	Cl	F	S	CH ₂ C ₆ H ₅	0	0	0	100	100	100
7an	150	Cl	F	S	CH ₂ C ₆ H ₄ (2-COOCH ₃)	0	0	0	80	70	50
7ao	150	Cl	F	S	CH ₂ COOCH ₃	50	100	100	100	100	100
7ap	150	Cl	F	S	CH ₂ COOCH ₂ CH ₃	70	90	100	100	100	100
7aq	150	Cl	F	S	CH ₂ COOCH(CH ₃) ₂	70	100	100	100	100	100
7ar	150	Cl	F	S	CH(CH ₃)COOCH ₃	90	100	100	100	100	100
(rac)-7as	150	Cl	F	S	CH(CH ₃)COOCH ₂ CH ₃	100	100	100	100	100	100
	75					90	100	100	100	100	100
	37.5					70	90	100	100	100	100
	18.75					60	80	90	100	100	100
(R)-7as	18.75					70	85	95	100	100	100
(S)-7as	18.75					60	80	90	100	100	100
7at	150	Cl	F	S	CH ₂ CH ₂ COOCH ₂ CH ₃	50	60	100	100	100	100
7au	150	Cl	F	S	CH(CH ₂ CH ₃)COOCH ₃	90	100	100	100	100	100
7av	150	Cl	F	S	CH(CH ₂ CH ₃)COOCH ₂ CH ₃	90	100	100	100	100	100
7aw	150	Cl	F	S	CH(CH ₂ CH ₃)COOCH ₂ CH ₃	40	50	100	100	100	100
7ax	150	Cl	F	S	CH ₂ CHCHCOOCH ₂ CH ₃	20	70	100	100	100	100
7ay	150	H	F	S	CH ₂ CH ₂ CH ₃	0	0	10	40	30	0
7az	150	H	F	S	CH ₂ COOCH ₂ CH ₃	0	20	30	100	80	70
7ba	150	H	F	S	CH(CH ₃)COOCH ₂ CH ₃	0	60	30	100	100	80
7bb	150	Cl	Cl	S	CH ₂ CH ₂ CH ₃	0	10	10	50	30	20
7bc	150	Cl	Cl	S	CH ₂ CH=CHCl	0	10	0	10	10	10
7bd	150	Cl	Cl	S	CH ₂ COOCH ₂ CH ₃	0	40	30	100	90	80
7be	150	Cl	Cl	S	CH(CH ₃)COOCH ₂ CH ₃	0	30	40	100	100	90
7bf	150	Cl	CH ₃	S	CH ₂ CH ₂ CH ₃	0	0	0	10	10	10
7bg	150	Cl	CH ₃	S	CH ₂ CH=CHCl	0	0	0	10	10	0
7bh	150	Cl	CH ₃	S	CH ₂ COOCH ₂ CH ₃	0	20	20	50	20	40
7bi	150	Cl	CH ₃	S	CH(CH ₃)COOCH ₂ CH ₃	0	20	30	50	20	40
8	150	Cl	F	SO ₂	CH ₃	0	0	10	30	30	0
9a	150	Cl	F	O	CH ₂ COOCH ₃	0	60	70	100	100	90
	75					0	20	40	100	70	80
9b	150	Cl	F	O	CH(CH ₃)COOCH ₃	0	60	70	100	100	90
	75					0	30	50	100	70	80
FLU ^b	150					90	100	100	100	100	100
	75					70	90	100	100	100	100
	37.5					50	80	90	100	100	100
	18.75					30	60	70	100	100	100

Table 1. continued

compd	dosage (g ai/ha)	X	Y	W	R	inhibition (%)					
						L.P. ^a	E.C.	D.S.	A.R.	A.T.	M.S.
SAF ^c	150					90	100	100	100	100	100
	75					80	100	95	100	100	100
	37.5					60	90	85	100	100	100
	18.75					40	85	80	100	100	100

^aAbbreviations: *Lolium perenne* (L.P.); *Echinochloa crusgalli* (E.C.); *Digitaria sanguinalis* (D.S.); *Amaranthus retroflexus* (A.R.); *Abutilon theophrasti* (A.T.); *Medicago sativa* (M.S.). ^bFlumioxazin (FLU). ^cSaflufenacil (SAF).

Table 2. Postemergence Crop Selectivities of Compounds 7ac, 7aj, and 7as, Flumioxazin and Saflufenacil

compd	dosage (g ai/ha)	crop injury (%)					
		rice	wheat	maize	peanut	cotton	soybean
7ac	150	15	20	20	15	100	30
	75	10	10	10	10	85	10
7aj	150	20	20	50	30	100	40
	75	10	10	40	20	90	20
(R)-7as	150	80	70	70	60	100	100
	75	70	60	50	50	100	90
(rac)-7as	150	70	40	60	50	100	100
	75	40	20	40	40	90	70
(S)-7as	150	65	35	55	40	100	100
	75	35	20	35	30	85	65
flumioxazin	150	80	75	70	80	100	100
	75	60	60	50	60	90	85
saflufenacil	150	80	60	75	90	100	100
	75	70	40	60	70	100	90

50 ps, followed by a 50 ps equilibration calculation at 1 atm and 300 K. Subsequently, a 20 ns molecular dynamics (MD) simulation was conducted for each complex. The snapshots captured during the final 10 ns of the MD simulation were employed for calculating the binding free energy. Finally, the root-mean-square deviation (RMSD) was used to evaluate the binding stability of the complexes of compounds 7aj, (R)-7as, and (S)-7as with NtPPO; the energy decomposition analysis for each system was executed utilizing the MM_PBSA module.

RESULTS AND DISCUSSION

Chemistry. As shown in Figure 2, intermediates 3a–3d were synthesized in moderate yields through Suzuki coupling reactions between the corresponding 2-chloropyridines (1a–1b) and phenylboronic acids (2a–2c) in the presence of Pd(Ph₃)₂Cl₂ as the catalyst. The nitro group was site-selectively installed through the nitration reaction, and the resulting compounds 4a–4d were used directly for the next reduction step without purification. Crude products 4a–4d were subjected to a mixture of Fe and NH₄Cl in ethanol/water (4:1), which subsequently were heated to reflux to yield the corresponding reduced amine products 5a–5d. Benzothiazoles 6a–6d were obtained by the reaction of 5a–5d and potassium ethyl xanthate in DMF at 90 °C via a cyclization process. After the reaction, hydrochloric acid was added to precipitate the products as a solid, and the desired product was isolated through vacuum filtration. Finally, intermediates 6a–6d were subjected to react with various halogenated compounds in the presence of K₂CO₃ as the base and CH₃CN as the solvent under 50 °C, which eventually results in the formation of the final products 7aa–7bi. The compounds (R)-7as and (S)-7as were prepared according to the previously reported method.³³ L-Alanine ethyl ester hydrochloride was dissolved in an aqueous solution of HBr (48%), and sodium nitrite aqueous

solution was slowly added dropwise at 0–5 °C. The mixture was stirred at 0–5 °C for 2 h to give (R)-2-bromo propionic acid ethyl ester. Replacing the L-alanine ethyl ester hydrochloride with D-alanine ethyl ester hydrochloride led to the formation of the (S)-2-bromo propionic acid ethyl ester. The compounds (R)-7as and (S)-7as were prepared by classical nucleophilic substitution reactions between 6a and the corresponding α-bromine carboxylic acid esters according to a reported method.³⁴ The enantiomeric excess (er) was determined by HPLC (for more detailed information, see Supporting Information).

To investigate the contribution of the sulfur atom in 7 to the herbicidal activity, the sulfur atom was changed to the oxygen atom via a sequence treatment of 7aa, including oxidation of 7aa and nucleophilic substitution with different alcohols, which eventually afford the target ethers 9a–9b. The chemical structures of the target compounds were characterized by ¹H, ¹³C, and ¹⁹F NMR spectra as well as HPLC and HRMS spectra.

Herbicidal Activity and Structure–Activity Relationship (SAR). The postemergence herbicidal activities of all the target compounds against six representative weeds were evaluated in a greenhouse environment. The PPO herbicides FLU and SAF were chosen as the control agents, and the evaluated data are presented in Table 1. Furthermore, when the tested weeds were exposed to light in the greenhouse, some of them displayed bleaching symptoms comparable to those caused by FLU or SAF. This confirmed that the synthesized target molecules functioned as PPO inhibitors (Figure 3). In the majority of instances, the herbicidal activities correlated with the inhibitory effects observed in in vitro experiments against AtPPO. As shown in Table 1, a large number of compounds such as 7ac–7aj, 7am, and 7ao–7ax exhibited

complete control against the three tested broad-leaved weeds at a dosage of 150 g ai/ha through postemergence application. Among them, compounds (*rac*)-7as, 7au, and 7av exhibited efficacy exceeding 90% against all six tested weeds at a dosage of 150 g of ai/ha. To have a clear understanding of the herbicidal activity of our target compounds, the postemergence herbicidal activities of 7ac, 7aj, and (*rac*)-7as were investigated at doses ranging from 18.75 to 75 g ai/ha. It is worth noting that compounds 7ac, 7aj, and (*rac*)-7as maintained their ability to completely control all the tested broadleaf weeds even at a dosage as low as 18.75 g ai/ha. The influence of the absolute configuration of 7as on the herbicidal activities was also explored. All three forms of compound 7as exhibited superior herbicidal activities against all of the tested weeds at a dosage of 18.75 g ai/ha to the commercial FLU. However, no significant difference in herbicidal activities was observed among (*rac*)-7as, (*R*)-7as, and (*S*)-7as under visual observation.

We then explored the structure–activity relationship (SAR) of 6-(substituted pyridin-2-yl)benzo[d]thiazole derivatives. The postemergence herbicidal activities of 6a–6d with different groups at X and Y positions were first investigated. The results showed that the substituents at X and Y may potentially alter the herbicidal spectrum of the target compound within a certain range (Table 1). For example, compound 6a (X = Cl, Y = F) exhibits a stronger herbicidal activity against broadleaf weeds compared to 6b–6d at a rate of 150 g ai/ha. Specifically, compound 6a exhibits herbicidal activities exceeding 80% against the three tested broadleaf weeds, whereas compounds 6b–6d showed weak herbicidal activities at a rate of 150 g ai/ha. It is worth noting that compounds 6a–6d do not exhibit any herbicidal activity against grassy weeds.

Subsequently, the effect of the substituent at the R position on the herbicidal activity was investigated using compounds 7aa–7bi as testing candidates, and the results are summarized in Table 1. Their herbicidal activity and spectrum were significantly superior to those of compound 6. For instance, the incorporation of $-\text{CH}_2\text{CH}_2\text{CH}_3$ (7ac) and $-\text{CH}_2\text{CCH}$ (7aj) as R groups significantly enhanced the herbicidal activity and expanded the herbicidal spectrum compared with other alkyl groups. The steric effect of the R group has a remarkable effect on the herbicidal activities as the herbicidal activities significantly decreased when bulky groups such as benzyl (7am) and 2-substituted benzyl (7an) were introduced as the R group. The incorporation of an ester group as the R moiety (7ao–7ba) significantly improved the herbicidal activities against both broadleaf weeds and grassy weeds. Besides, the steric effect of this ester group also has a remarkable effect on the herbicidal activities. Among all of the tested R groups, $-\text{CH}(\text{CH}_3)\text{COOC}_2\text{H}_5$ (7as) showed optimal activities against all of the tested broadleaf weeds and grassy weeds. To investigate the influence of the absolute configuration of 7as on the herbicidal activities, the herbicidal activities of (*rac*)-7as, (*R*)-7as, and (*S*)-7as were evaluated, respectively, at a dosage of 18.5 g ai/ha. The results suggested that the absolute configuration did not significantly affect the herbicidal activity (Table 1). However, it is worth noting that compound (*R*)-7as exhibited faster burning symptoms on the leaves during the initial test stage compared to those of (*rac*)-7as and (*S*)-7as. In addition, replacing the sulfur atom with SO_2 will decrease the herbicidal effectiveness. For example, the herbicidal activities of compound 7aa were significantly greater than that of compound 8. Similarly, replacing the S atom with the O

atom also resulted in a significant loss of herbicidal efficacy, as the herbicidal activities of compounds 7ao and 7ar were notably higher than those of compounds 9a and 9b.

Based on the above analysis, we conclude that the R group has a significant impact on the herbicidal activities and the introduction of the ester group as the R moiety can significantly improve the herbicidal activities. Among the tested ester groups, $-\text{CH}(\text{CH}_3)\text{COOC}_2\text{H}_5$ exhibited the highest herbicidal activity. The order for other groups is alkyl, benzyl, or hydrogen atoms (ester group > alkyl > benzyl \approx hydrogen). The SAR results mentioned above are shown in Figure 5.

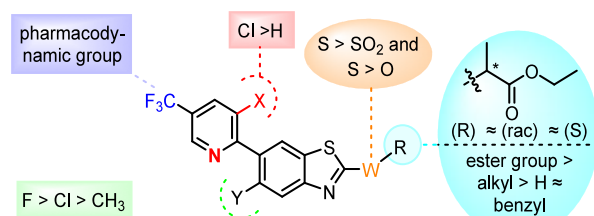


Figure 5. SAR analysis of 6-(substituted pyridin-2-yl)benzo[d]thiazole derivatives as herbicides.

Crop Selectivity. As an effort to further explore the potential of the highly active 6-(substituted pyridin-2-yl)benzo[d]thiazole derivatives as herbicide candidates, we evaluated the postemergence crop safety of representative compounds 7ac, 7aj, (*rac*)-7as, (*R*)-7as, and (*S*)-7as at dosages ranging from 75 to 150 g ai/ha. As detailed in Table 2, in most cases, all of our tested compounds exhibited better crop safety than the commercially available FLU and SAF. Specifically, compounds 7ac and 7aj exhibited the highest crop safety to rice, wheat, corn, and peanut. The crop safety of compound 7as is limited, whereas it is still better than FLU and SAF, and it exhibited a specific selectivity for wheat. Furthermore, although the absolute configuration of compound 7as has no obvious effect on its herbicidal activity, compound (*R*)-7as showed slightly higher crop safety than compound (*S*)-7as as plants treated with (*R*)-7as exhibited more pronounced symptoms of scorching in the early stages. However, it should be noted that no significant differences were observed in the later stages. From the perspective of the relationship between structure and activity, saturated (7ac) and unsaturated (7aj) thiol ethers exhibited better crop safety. In contrast, the introduction of an ester group damaged the selectivity for crops (*rac*)-7as. It is worth noting that the overall selectivity of all the tested compounds toward crops is higher than that of FLU, indicating that compound (*rac*)-7as holds significant potential for developing novel herbicides.

PPO Inhibitory Activity. As shown in Table 3, several representative compounds with high herbicidal activity were subjected to *in vitro* experiments to evaluate their inhibition for the AtPPO enzyme. The results suggested that some of our compounds exhibited superior inhibition against AtPPO to the commercial herbicide FLU ($\text{IC}_{50} = 0.94 \mu\text{M}$). For example, 7ag ($\text{IC}_{50} = 0.06 \mu\text{M}$), 7am ($\text{IC}_{50} = 0.26 \mu\text{M}$), 7at ($\text{IC}_{50} = 0.11 \mu\text{M}$), and 8 ($\text{IC}_{50} = 0.30 \mu\text{M}$) showcased a higher inhibitory activity than FLU ($\text{IC}_{50} = 0.94 \mu\text{M}$). It has been proven that the substituent at the R position has a significant influence on the AtPPO enzyme inhibitory activity. For instance, the inhibitory activity of compound 7aa (R = CH_3 , $\text{IC}_{50} = 0.95$

Table 3. *At*PPO Inhibitory Activity of Representative Substituted 6-(pyridin-2-yl) Benzothiazole Derivatives and Flumioxazin

compd	IC ₅₀ (μM)	compd	IC ₅₀ (μM)
6a	0.40	(<i>rac</i>)-7as	0.30
7aa	0.95	(<i>R</i>)-7as	0.23
7ac	0.73	(<i>S</i>)-7as	1.36
7ag	0.06	7at	0.11
7ai	0.28	7ax	0.30
7aj	0.72	7ba	0.23
7am	0.26	7be	0.30
7ao	0.68	7bi	0.47
7ap	0.27	8	0.30
7aq	0.46	9b	0.80
7ar	0.55	flumioxazin	0.94

μM) to the *At*PPO enzyme is lower than those of compounds 7ac (R = CH₂CH₂CH₃, IC₅₀ = 0.73 μM) and 7aj (R = CH₂C≡CH, IC₅₀ = 0.72 μM), which is consistent with their herbicidal activities. The higher inhibitory activity of compounds 7ag (R = CH₂CH = CH₂, IC₅₀ = 0.06 μM) and 7ai (R = CH₂CH = CHCl, IC₅₀ = 0.28 μM) may be attributed to the introduction of double bonds and the chlorine atom, which may contribute to the toxic property.

In terms of ester-containing compounds, a correlation between the inhibitory activity against *At*PPO and the herbicidal activity was observed. For example, the *At*PPO inhibitory activity of compound 7as (IC₅₀ = 0.30 μM) that exhibited the highest herbicidal activity was greater than that of 7ao (IC₅₀ = 0.68 μM), 7aq (IC₅₀ = 0.46 μM), and 7ar (IC₅₀ = 0.55 μM). The difference in the inhibition rates of 7ao–7ax on *At*PPO may be attributed to the different ester groups, which lead to complex interactions between the side chains and the protein.

The substituent at positions X and Y had a slight effect on the inhibitory activity against *At*PPO. For example, compounds 7ba (X = H, IC₅₀ = 0.23 μM) exhibited a slightly higher

inhibitory activity than 7as (X = Cl, IC₅₀ = 0.30 μM). Fluorine (7as, Y = F, IC₅₀ = 0.30 μM) and chlorine atom (7be, Y = Cl, IC₅₀ = 0.30 μM) containing compounds showed a higher inhibitory activity against *At*PPO than the methyl-substituted one (7bi, Y = CH₃, IC₅₀ = 0.47 μM). This structure–activity relationship demonstrated that the electron-withdrawing groups at the Y position contribute more to the inhibitory activity against *At*PPO than do the electron-donating ones. Meanwhile, compound (*R*)-7as (IC₅₀ = 0.23 μM) exhibited a higher inhibition rate against PPO compared to (*rac*)-7as (IC₅₀ = 0.30 μM) and (*S*)-7as (IC₅₀ = 1.36 μM), which may explain the symptomatology (compound (*R*)-7as exhibited faster burning symptoms on the leaves during the initial test stage) observed in the herbicidal testing. When the sulfur atom was replaced by the sulfone group, compound 8 (W=SO₂, IC₅₀ = 0.30 μM) also exhibited a high inhibitory activity against *At*PPO. In contrast, the replacement of sulfur atom by oxygen atom (9b, W=O, IC₅₀ = 0.94 μM) led to a decreased inhibitory activity.

Molecular Simulation Studies. To gain insights into the inhibitory mechanism at the molecular level, molecular simulation studies were employed to investigate the interactions between our compounds and *Nt*PPO (Figure 6). A π–π stacking interaction between the benzene ring of Phe-392 and the pyridine ring of compound 7aj was observed with a bond length of 3.9 Å. Besides, a π–π interaction with a bond length of 4.2 Å formed between the thiazole moiety and Phe-353. In terms of 7as, a quadruple π–π interaction between the benzothiazole moiety of (*R*)-7as and FAD was observed. Besides, the pyridine ring of (*R*)-7as generated π–π stacking with Phe-392. The results demonstrated that the benzothiazole moiety of (*R*)-7as is closer to the flavin adenine dinucleotide (FAD) when compared to compound 7aj, resulting in stronger and multiple interactions. The influence of the absolute configuration on the interactions between 7as and *Nt*PPO was investigated. It was found that while (*S*)-7as underwent an overall inversion in position relative to (*R*)-7as, it exhibits

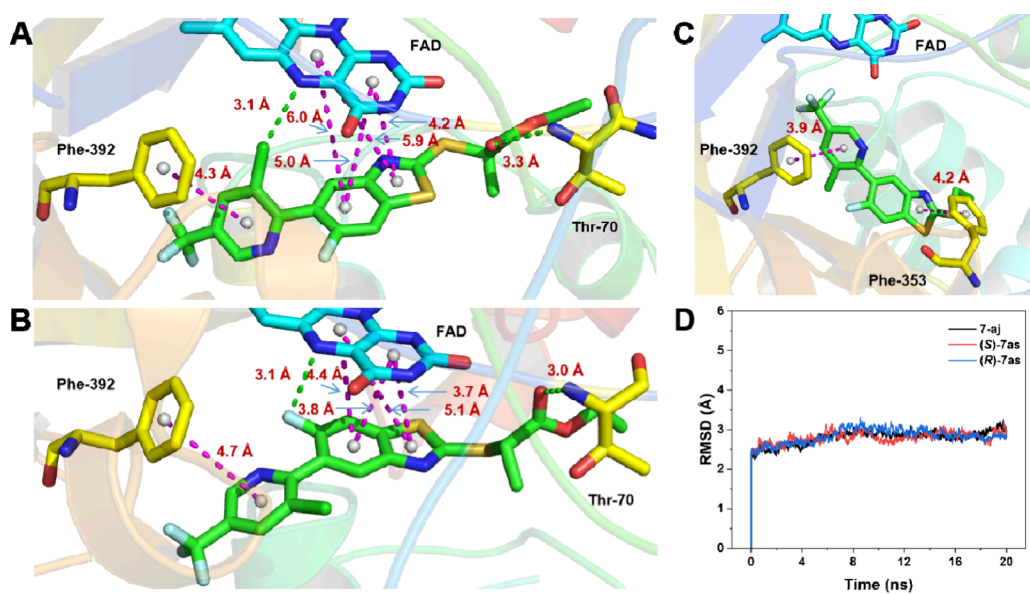


Figure 6. Simulated binding modes of compounds (A–C) (*R*)-7as, (*S*)-7as, and 7aj, with *Nt*PPO after 20 ns of MD simulation. The compounds (*R*)-7as, (*S*)-7as, and 7aj are shown as green sticks. The key residues around the active site are shown as yellow sticks. FAD is shown as blue sticks. (D) RMSD of backbone atoms of the protein.

similar interactions with *Nt*PPO, which is consistent with the similar herbicidal activities of (*S*)-7as and (*R*)-7as.

Based on the results of MD simulation, as shown in Figure 6D, over a 20 ns MD simulation period, all root-mean-square-deviation (RMSD) values of backbone atoms of *Nt*PPO protein are in the range 2.5–3.0 Å at the last 10 ns, indicating that the 7aj-*Nt*PPO, (*R*)-7as-*Nt*PPO, and (*S*)-7as-*Nt*PPO systems have reached stability. To further understand the contribution of each amino acid residue around the active site cavity, the results are shown in Figure 7. The results of energy

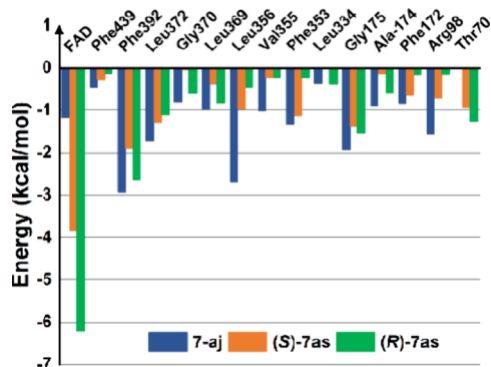


Figure 7. Decomposition of the binding free energy (kcal/mol) between compounds (*R*)-7as, (*S*)-7as, and 7aj and *Nt*PPO.

decomposition studies of the 7aj, (*R*)-7as, and (*S*)-7as-*Nt*PPO systems indicated that the introduction of an ester group resulted in an enhanced energy contribution of FAD compared to the alkyl group. In addition, it was found that Phe-392, Leu-356, and Gly-175 make the primary energy contributions in the 7aj-*Nt*PPO system, which is similar to the (*R*)-7as and (*S*)-7as-*Nt*PPO systems. Meanwhile, the hydrophobic contact interactions between (*R*)-7as or (*S*)-7as and FAD, Phe392, Leu356, Phe353, and Gly175 also significantly contribute to the binding free energies. These computational data once again demonstrate the potential of 6-(substituted pyridin-2-yl)benzo[d]thiazole derivatives as novel PPO inhibitors.

In summary, we have designed a series of structurally novel 6-(pyridin-2-yl) benzothiazole derivatives as novel PPO inhibitors under the direction of a scaffold hopping strategy. Systematic herbicidal activity evaluations of the synthesized 42 target compounds revealed that some of them such as 7ac, 7aj, (*rac*)-7as, (*R*)-7as, and (*S*)-7as exhibited good-to-excellent herbicidal activity against the tested broadleaf weeds and grassy weeds even at a dosage as low as 18.75 g ai/ha. Crop selectivity studies demonstrated that these compounds also exhibited higher crop safety compared to the control agent FLU. The absolute configuration of compound 7as had a minimal impact on herbicidal activity and crop selectivity. The *in vitro* inhibition experiments showed that the majority of compounds exhibited IC_{50} values in the nmol range against the *At*PPO enzyme. Molecular docking results indicated that the benzothiazole moiety of our compounds formed multiple π - π stacking interactions with FAD, and the pyridine ring also potentially engaged in a π - π interaction with Phe-392 in *Nt*PPO. Our current research not only provides a series of potential candidate compounds for herbicide discovery but also offers a valuable example of applying a scaffold hopping strategy in the design of new biologically active compounds.

■ ASSOCIATED CONTENT

Supporting Information

The Supporting Information is available free of charge at <https://pubs.acs.org/doi/10.1021/acs.jafc.3c08596>.

Characterization data, 1H , ^{13}C , ^{19}F NMR spectra, HPLC spectra, HRMS spectra for intermediates and title compounds are provided (PDF)

Crystal Structure of Rac-7as (CIF)

■ AUTHOR INFORMATION

Corresponding Authors

Shi-Chao Ren – National Key Laboratory of Green Pesticide, Key Laboratory of Green Pesticide and Agricultural Bioengineering, Ministry of Education, Guizhou University, Guiyang 550025, China; orcid.org/0000-0003-4248-6021; Email: sren@gzu.edu.cn

Yonggui Robin Chi – National Key Laboratory of Green Pesticide, Key Laboratory of Green Pesticide and Agricultural Bioengineering, Ministry of Education, Guizhou University, Guiyang 550025, China; School of Chemistry, Chemical Engineering, and Biotechnology, Nanyang Technological University, Singapore 637371, Singapore; orcid.org/0000-0003-0573-257X; Email: robinchi@ntu.edu.sg

Authors

Hui Cai – National Key Laboratory of Green Pesticide, Key Laboratory of Green Pesticide and Agricultural Bioengineering, Ministry of Education, Guizhou University, Guiyang 550025, China

Xiao Zhang – National Key Laboratory of Green Pesticide, Key Laboratory of Green Pesticide and Agricultural Bioengineering, Ministry of Education, Guizhou University, Guiyang 550025, China

Dan Ling – National Key Laboratory of Green Pesticide, Key Laboratory of Green Pesticide and Agricultural Bioengineering, Ministry of Education, Guizhou University, Guiyang 550025, China

Meng Zhang – National Key Laboratory of Green Pesticide, Key Laboratory of Green Pesticide and Agricultural Bioengineering, Ministry of Education, Guizhou University, Guiyang 550025, China

Chen Pang – National Key Laboratory of Green Pesticide, Key Laboratory of Green Pesticide and Agricultural Bioengineering, Ministry of Education, Guizhou University, Guiyang 550025, China

Zhongyin Chen – National Key Laboratory of Green Pesticide, Key Laboratory of Green Pesticide and Agricultural Bioengineering, Ministry of Education, Guizhou University, Guiyang 550025, China

Zhichao Jin – National Key Laboratory of Green Pesticide, Key Laboratory of Green Pesticide and Agricultural Bioengineering, Ministry of Education, Guizhou University, Guiyang 550025, China

Complete contact information is available at: <https://pubs.acs.org/doi/10.1021/acs.jafc.3c08596>

Notes

The authors declare no competing financial interest.

■ ACKNOWLEDGMENTS

We acknowledge financial support from the National Natural Science Foundation of China (22371058, 21961006,

32172459, 22371057, and 22071036), the National Key Research and Development Program of China (2022YFD1700300), the Science and Technology Department of Guizhou Province (Qiankehejichu-ZK[2021]Key033), the Program of Introducing Talents of Discipline to Universities of China (111 Program, D20023) at Guizhou University, Frontiers Science Center for Asymmetric Synthesis and Medicinal Molecules, Department of Education, Guizhou Province [Qianjiaohu KY (2020)004], and Guizhou University (China).

ABREVIATIONS

AtPPO, *Arabidopsis thaliana* PPO; NtPPO, *Nicotiana tabacum* PPO; FLU, flumioxazin; SAF, saflufenacil; MD, molecular dynamics; IC₅₀, half-maximal inhibitory concentration; ROS, reactive oxygen species; ESP, electrostatic potential; NMR, nuclear magnetic resonance; SARs, structure–activity relationships; HRMS, high-resolution mass spectrum; *L.P.*, *Lolium perenne*; *E.C.*, *Echinochloa crusgalli*; *D.S.*, *Digitaria sanguinalis*; *A.R.*, *Amaranthus retroflexus*; *A.T.*, *Abutilon theophrasti*; *M.S.*, *Medicago sativa*; DMF, N,N-dimethylformamide; THF, tetrahydrofuran.

REFERENCES

- (1) Zhang, F.; Tang, W.; Hedtke, B.; Zhong, L.; Liu, L.; Peng, L.; Lu, C.; Grimm, B.; Lin, R. Tetrapyrrole biosynthetic enzyme protoporphyrinogen IX oxidase 1 is required for plastid RNA editing. *Proc. Natl. Acad. Sci. U. S. A.* **2014**, *111*, 2023–2028.
- (2) Wang, P.; Ji, S.; Grimm, B. Post-translational regulation of metabolic checkpoints in plant tetrapyrrole biosynthesis. *J. Exp. Bot.* **2022**, *73*, 4624–4636.
- (3) Wang, B.; Wen, X.; Xi, Z. Molecular simulations bring new insights into protoporphyrinogen IX oxidase/protoporphyrinogen IX interaction modes. *Mol. Inform.* **2016**, *35*, 476–482.
- (4) Hao, G.-F.; Zuo, Y.; Yang, S.-G.; Chen, Q.; Zhang, Y.; Yin, C.-Y.; Niu, C.-W.; Xi, Z.; Yang, G.-F. Computational discovery of potent and bioselective protoporphyrinogen IX oxidase inhibitor via fragment deconstruction analysis. *J. Agric. Food Chem.* **2017**, *65*, 5581–5588.
- (5) Zheng, B.-F.; Wang, Z.-Z.; Dong, J.; Ma, J.-Y.; Zuo, Y.; Wu, Q.-Y.; Yang, G.-F. Discovery of a subnanomolar inhibitor of protoporphyrinogen IX oxidase via fragment-based virtual screening. *J. Agric. Food Chem.* **2023**, *71*, 8746–8756.
- (6) Rangani, G.; Salas-Perez, R. A.; Aponte, R. A.; Knapp, M.; Craig, I. R.; Mietzner, T.; Langaro, A. C.; Noguera, M. M.; Porri, A.; Romaburgos, N. A novel single-site mutation in the catalytic domain of protoporphyrinogen oxidase IX (PPO) confers resistance to PPO-inhibiting herbicides. *Front. Plant Sci.* **2019**, *10*, 568–579.
- (7) Ambrosini, V.; Issawi, M.; Leroy-Lhez, S.; Riou, C. How protoporphyrinogen IX oxidase inhibitors and transgenesis contribute to elucidate plant tetrapyrrole pathway. *J. Porphyr. Phthalocya.* **2019**, *23*, 419–426.
- (8) Dayan, F. E.; Barker, A.; Tranel, P. J. Origins and structure of chloroplast and mitochondrial plant protoporphyrinogen oxidases: implications for the evolution of herbicide resistance. *Pest Manag. Sci.* **2018**, *74*, 2226–2234.
- (9) Brzezowski, P.; Ksas, B.; Havaux, M.; Grimm, B.; Chazaux, M.; Peltier, G.; Johnson, X.; Alric, J. The function of protoporphyrinogen IX oxidase in chlorophyll biosynthesis requires oxidised plastoquinone in *Chlamydomonas reinhardtii*. *Commun. Biol.* **2019**, *2*, 159–168.
- (10) Zhao, L.-X.; Chen, K.-Y.; He, X.-L.; Zou, Y.-L.; Gao, S.; Fu, Y.; Ye, F. Design, synthesis, and biological activity determination of novel phenylpyrazole protoporphyrinogen oxidase inhibitor herbicides containing five-membered heterocycles. *J. Agric. Food Chem.* **2023**, *71*, 14164–14178.
- (11) Wang, D.-W.; Li, Q.; Wen, K.; Ismail, I.; Liu, D.-D.; Niu, C.-W.; Wen, X.; Yang, G.-F.; Xi, Z. Synthesis and herbicidal activity of pyrido[2,3-d]pyrimidine-2,4-dione–benzoxazinone hybrids as protoporphyrinogen oxidase inhibitors. *J. Agric. Food Chem.* **2017**, *65*, 5278–5286.
- (12) Giacomini, D. A.; Umphres, A. M.; Nie, H.; Mueller, T. C.; Steckel, L. E.; Young, B. G.; Scott, R. C.; Tranel, P. J. Two new PPX2 mutations associated with resistance to PPO-inhibiting herbicides in *Amaranthus palmeri*. *Pest Manag. Sci.* **2017**, *73*, 1559–1563.
- (13) Zhao, L.-X.; Peng, J.-F.; Liu, F.-Y.; Zou, Y.-L.; Gao, S.; Fu, Y.; Ye, F. Discovery of novel phenoxypyridine as promising protoporphyrinogen IX oxidase inhibitors. *Pest. Biochem. Physiol.* **2022**, *184*, 105102–105111.
- (14) Wang, D. W.; Liang, L.; Xue, Z. Y.; Yu, S. Y.; Zhang, R. B.; Wang, X.; Xu, H.; Wen, X.; Xi, Z. Discovery of N-Phenylaminomethylthioacetylpyrimidine-2,4-diones as protoporphyrinogen IX oxidase inhibitors through a reaction intermediate derivation approach. *J. Agric. Food Chem.* **2021**, *69*, 4081–4092.
- (15) Qu, R. Y.; He, B.; Yang, J. F.; Lin, H. Y.; Yang, W. C.; Wu, Q. Y.; Li, Q. X.; Yang, G. F. Where are the new herbicides? *Pest Manag. Sci.* **2021**, *77*, 2620–2625.
- (16) Wang, D.-W.; Zhang, R.-B.; Ismail, I.; Xue, Z.-Y.; Liang, L.; Yu, S.-Y.; Wen, X.; Xi, Z. Design, herbicidal activity, and QSAR analysis of cycloalka[d]quinazoline-2,4-dione–benzoxazinones as protoporphyrinogen IX oxidase inhibitors. *J. Agric. Food Chem.* **2019**, *67*, 9254–9264.
- (17) Nie, H.; Mansfield, B. C.; Harre, N. T.; Young, J. M.; Steppig, N. R.; Young, B. G. Investigating target-site resistance mechanism to the PPO-inhibiting herbicide fomesafen in waterhemp and interspecific hybridization of *Amaranthus* species using next generation sequencing. *Pest Manag. Sci.* **2019**, *75*, 3235–3244.
- (18) Sun, H.; Tawa, G.; Wallqvist, A. Classification of scaffold-hopping approaches. *Drug Discovery Today* **2012**, *17*, 310–324.
- (19) Zhang, P.; Duan, C.-B.; Jin, B.; Ali, A. S.; Han, X.; Zhang, H.; Zhang, M.-Z.; Zhang, W.-H.; Gu, Y.-C. Recent advances in the natural products-based lead discovery for new agrochemicals. *Adv. Agrochem* **2023**, *2*, 324–339.
- (20) Barber, D. M. A competitive edge: competitor inspired scaffold hopping in herbicide lead optimization. *J. Agric. Food Chem.* **2022**, *70* (36), 11075–11090.
- (21) Yang, X.; Wang, H.; Jin, Z.; Chi, Y. R. Development of green and low-cost chiral oxidants for asymmetric catalytic hydroxylation of enals. *Green Synth. Catal.* **2021**, *2*, 295–298.
- (22) Lv, Y.; Luo, G.; Liu, Q.; Jin, Z.; Zhang, X.; Chi, Y. R. Catalytic atroposelective synthesis of axially chiral benzonitriles via chirality control during bond dissociation and CN group formation. *Nat. Commun.* **2022**, *13*, 36–45.
- (23) Tang, C.; Wang, W.; Luo, G.; Song, C.; Bao, Z.; Li, P.; Hao, G.; Chi, Y. R.; Jin, Z. *Angew. Chem., Int. Ed.* **2022**, *61*, No. e2022069.
- (24) Wang, D. W.; Zhang, R. B.; Yu, S. Y.; Liang, L.; Ismail, I.; Li, Y. H.; Xu, H.; Wen, X.; Xi, Z. Discovery of novel N-isoxazolylphenyltriazinones as promising protoporphyrinogen IX oxidase inhibitors. *J. Agric. Food Chem.* **2019**, *67*, 12382–12392.
- (25) Zuo, Y.; Wu, Q.; Su, S. W.; Niu, C. W.; Xi, Z.; Yang, G. F. Synthesis, herbicidal activity, and QSAR of novel N-benzothiazolylpyrimidine-2,4-diones as protoporphyrinogen oxidase inhibitors. *J. Agric. Food Chem.* **2016**, *64*, 552–562.
- (26) Schäfer, P.; Hamprecht, G.; Puhl, M.; Westphalen, K. O.; Zagar, C. Synthesis and herbicidal activity of phenylpyridines—a new lead. *Chimia* **2003**, *57*, 715–719.
- (27) Bauer, M. R.; Mackey, M. D. Electrostatic complementarity as a fast and effective tool to optimize binding and selectivity of protein–ligand complexes. *J. Med. Chem.* **2019**, *62*, 3036–3050.
- (28) Cons, B. D.; Twigg, D. G.; Kumar, R.; Chessari, G. Electrostatic complementarity in structure-based drug design. *J. Med. Chem.* **2022**, *65* (11), 7476–7488.
- (29) Wang, Y.; Xiong, Y.; Garcia, E. A. L.; Wang, Y.; Butch, C. J. Drug chemical space as a guide for new herbicide development: a cheminformatic analysis. *J. Agric. Food Chem.* **2022**, *70* (31), 9625–9636.

(30) Zhao, L.-X.; Wang, Z.-X.; Zou, Y.-L.; Gao, S.; Fu, Y.; Ye, F. Phenoxypyridine derivatives containing natural product coumarins with allelopathy as novel and promising protoporphyrin IX oxidase-inhibiting herbicides: Design, synthesis and biological activity study. *Pest. Biochem. Physiol.* **2021**, *177*, No. 104897.

(31) Zheng, B.-F.; Zuo, Y.; Huang, G.-Y.; Wang, Z.-Z.; Ma, J.-Y.; Wu, Q.-Y.; Yang, G.-F. Synthesis and biological activity evaluation of benzoxazinone-pyrimidinedione hybrids as potent protoporphyrinogen IX oxidase inhibitor. *J. Agric. Food Chem.* **2023**, *71*, 14221–14231.

(32) Zhao, L.-X.; Peng, J.-F.; Liu, F.-Y.; Zou, Y.-L.; Gao, S.; Fu, Y.; Ye, F. Design, synthesis, and herbicidal Activity of diphenyl ether derivatives containing a five-membered heterocycle. *J. Agric. Food Chem.* **2022**, *70*, 1003–1018.

(33) Luehr, G. W.; Sundaram, A.; Jaishankar, P.; Payne, P. W.; Druzgala, P. d2 antagonists, methods of synthesis and methods of use. WO Patent WO2011160084, Dec. 22, 2011.

(34) Fleer, M. P. M.; Verkuil, B. J. V. Optimization of the use of a chiral bio-based building block for the manufacture of DHPPA, a key intermediate for propionate herbicides. *Green Chem.* **2014**, *16*, 3993–3998.